MICROVASCULAR TOPOLOGY AND INTRAVASCULAR ENDOTHELIAL CELL LABELING IN THE GRACILIS ANTERIOR MUSCLE OF BALB/C MICE

A Senior Project

Presented to

The Faculty of Biomedical and General Engineering Department

California Polytechnic State University,

San Luis Obispo

In Partial Fulfillment

Of the Requirements for the Degree

Bachelor of Science in Biomedical Engineering

by

Paul Heckler II

August 2014

TITLE: MICROVASCULAR TOPOLOGY AND INTRAVASCULAR ENDOTHELIAL CELL LABELING IN THE GRACILIS ANTERIOR MUSCLE OF BALB/C MICE

AUTHOR Paul Heckler II

DATE SUBMITTED: August 2014

ADVISOR Trevor Cardinal, Associate Professor

ABSTRACT

Microvascular Topology and Intravascular Endothelial Cell Labeling in the Gracilis Anterior Muscle of Balb/C Mice

Paul Henry Heckler II

Peripheral arterial occlusive disease (PAOD) affects approximately 200 million individuals globally. The major underlying cause of PAOD is an inflammatory disease known as atherosclerosis, which results from the build-up of low-density lipoproteins (LDL) in the sub-intimal space. This initiates a complex cascade of events that lead to plaque growth. Plaque growth can then expand into the lumen of the vessel and result in occlusion and/or thrombosis. Symptoms of the disease can include claudication, ulcers, and/or gangrene, although many patients are asymptomatic. Similar to other forms of ischemic disease, risk factors for PAOD include hypertension, diabetes, and smoking. Common treatments include life style changes, antiplatelet therapies, and endovascular and surgical revascularization. Natural bypass surgery is a common revascularization method for patients suffering from advanced stages of PAOD. In this procedure an autologous vein segment is grafted to bypass a section of occluded artery. However, many patients experience restenosis or are unable to undergo such an invasive procedure. New therapies are needed to bridge this gap in patient care. A natural bypass is a healing mechanism that takes advantage of pre-existing vessels by enlarging them to compensate for occluded flow in another vessel. The extent to which these natural bypasses can restore the original flow rate seems to be predicated on the vascular network topology of an individual. Animal studies indicate that microvascular topologies can be either protective or vulnerable to ischemic insult from ischemic diseases, such as PAOD. Mice with highly interconnected (anastomotic) vessel networks experience faster recovery times than those with branching tree –like (dendritic) structures, likely due to compensation mechanisms from redundant supply vessels. Balb/C mice mimic dendritic architecture and experience greater ischemia and reduced hind limb functionality compared with C57BL/6 mice, which are the anastomotic archetype, following hind limb femoral artery ligation. The presence of collateral vessels in the gracilis of Balb/C mice, observed in previous work and confirmed in this study provides evidence that preexisting collaterals alone are not sufficient for improving flow. Evaluating the ability of the gracilis collateral to re-perfuse the distal hindlimb would require perfusion labeling of the endothelium, such as with lectin. The technique for perfusion labeling the gracilis muscle was demonstrated in this study. Promising results were obtained, however further optimization will be needed to improve consistency of the labeling. These findings suggest further investigation into both the nature of impaired collateral remodeling, and the continued optimization of the of lectin perfusion labeling to asses re-perfusion following arterial occlusion.

Keywords: Angiogenesis, Arteriogenesis, Collateral, Morphology, Network, Vasodilation

Acknowledgements

I wish to thank the supportive guidance of Dr. Trevor Cardinal and the members of the Microcirculation lab. Special thanks to Jen Go, who provided assistance far beyond the call of duty. My parents also deserve the sincerest gratitude for their continued love and advocacy of my studies throughout the years.

“To myself I am only a child playing on the beach, while vast oceans of truth lie undiscovered before me.” — Isaac Newton

Table of Contents

List of Figures:

Introduction

Peripheral Artery Disease (PAOD) is broadly defined as the impaired function and/or structure of noncoronary arteries and it affects 27 million people in Western Europe and North America [3,7]. Clinical manifestations of PAOD include claudication, impaired mobility, ischemic pain at rest, and/or impaired wound recovery, although many patients with PAOD may be asymptomatic [3, 7, 2]. These symptoms are associated with decreased quality of life, limb amputations, and an increased risk of death because PAOD is generally an indicator of systemic atherosclerosis [1]. This paper will focus on the current understanding of PAOD, including its pathophysiology, current treatments, and novel research to improve patient therapies.

Atherosclerosis is a chronic disease of the artery wall that results in the formation of subintimal atheromatous lesions that can reduce lumen diameter and decrease or stop blood flow [4]. Conditions such as hypertension, which cause damage to the arterial wall, alone or in combination with turbulent sheer stress seen at arterial bifurcations, activates the endothelial layer to allow increased migration and retention of low-density lipoproteins (LDLs) into subintimal area [4]. The activated endothelial cells also present adhesion proteins that bind leukocytes, which extravasate into the subintimal area [4]. Extravasated monocytes transform into macrophages, which phagocytose LDL particles and eventually become foam cells [4]. This process initiates a positive feedback loop of inflammation that results in a fatty plaque build up. This build-up can result in obstruction of flow via stenosis and/or initiation of thrombi that blocks flow at or downstream of the plaque site [4]. The obstructed flow reduces nutrient delivery to tissue downstream, causing ischemia and/or cell death [4].

Diagnosising PAOD in patients is challenged by the lack of clinical presentation, making it difficult to identify at-risk patients [5]. One of the few easily identifiable symptoms is intermittent claudication, which is seen in conjunction with peripheral artery disease in 20-40% of patients [6]. Risk factors for the disease include: smoking, diabetes, hypertension, and hyperlipidemia [3, 7]. For at-risk patients and those over the age of 50, a non-invasive measurement known as the ankle-brachial pressure index (ABPI) test is administered to detect PAOD [6]. The ABPI is calculated by measuring the systolic blood pressure in the arterial vessels of the ankle, and dividing it by a measurement of the systolic pressure of the brachial artery. ABPI values range from healthy, anything greater than 1, to moderate disease, 0.5-0.80, to

critical ischemia, which is anything less than 0.30 [5]. Preventative/interventional lifestyle changes are recommended for patients with or at risk for disease. These changes can include exercise programs, cholesterol management drugs, smoking cessation, and anti-platelet therapies [6].

Advanced cases of PAOD, such as in the case of critical limb ischemia (CLI), may require revascularization procedures. These can include endovascular treatments and surgical revascularization [7]. Endovascular procedures are widely used as a first line of treatment, as percutaneous procedures involve less risk than surgical revascularization and can achieve limb salvage and viability [8]. Surgical revascularization is used for patients with extensive foot infections, tissue loss, or gangrene. These more advanced symptoms call for surgical revascularization because it can increase blood flow to the limb and allows for more intensive treatment, if necessary. Many of these patients however, are unable to receive treatment using traditional methods. These patients may be unable to sustain the rigors of surgery, lack of suitable vessels for use, or develop restenosis following a procedure [9]. Thus, there is a need for treatments that prevent and ameliorate symptoms resulting from PAOD, such as by promoting natural healing mechanisms and understanding genetic predispositions that affect the body's ability to recover from an occlusion.

Natural healing mechanisms, or endogenous vascularization, can be broken into angiogenesis and arteriogenesis. Angiogenesis is the sprouting of new capillaries from pre-existing vessels and results in the formation of new capillary networks [10]. It occurs during embryonic development and wound healing to supply tissue with necessary nutrients [11]. Initial attempts at reperfusing tissue through endogenous revascularization focused on stimulating angiogenesis, however clinical trials for these treatments have shown limited efficacy [18–20]. In light of these findings, emerging efforts have focused on arteriogenesis as an alternative method for restoring blood flow. Arteriogenesis describes the growth of functional collateral arteries from pre-existing arteriole-arteriole anastomoses, Figure 1 [10].

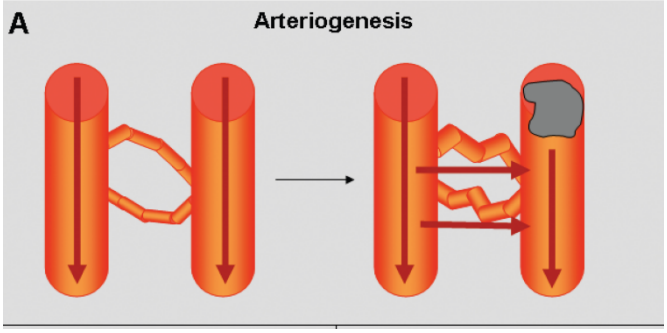

Figure 1. Enlargement of collateral vessels following occlusion of artery. The collateral vessels (smaller vessels perpendicular to arteries) undergo arteriogenesis in response to increased flow and shear stress. This enlarges the vessels and helps restore flow to the occluded artery [10].

Experimental data indicates that the driving force for arteriogenesis is shear stress [9]. The increased shear stress initiates a cascade of events that leads to increased vessel lumen diameter and wall thickness [10]. This means that unlike angiogenesis, which is stimulated by hypoxia, arteriogenesis can occur in the absence of hypoxic tissue. The reason why arteriogenesis is so effective at restoring flow can be seen by examining the Hagen-Poiseuille Equation, Equation 2. Holding all other variables constant the flow rate, Q, is dependent on the radius raised to the fourth power, meaning that even small increases in diameter can lead to large increases in flow rate. Both experimental and theoretical data indicate that arteriogenesis can play an important role in restoring flow in tissue following an occlusive event.

Equation 1: Hagen-Poiseuille Equation

$$Q = \frac{\pi R^4 \Delta P}{8\eta L}$$

Project Rationale

Recent efforts have focused on characterizing vascular network's acute and chronic responses to ischemic injury, to construct a model for natural healing mechanisms that accounts for both the role of both the physical network structure and the network's ability to adapt over time [14-15]. These networks are the transportation routes through which blood delivers oxygen and nutrients to tissue. Depending on the layout of these vascular networks, they can either be highly susceptible to tissue damage resulting from occlusions, or protected against it

[14-15]. Depending on the severity of the occlusion, symptoms can range from greater fatigue to necrosis and loss of limbs [1]. There is a strong interest in developing therapies that take adavantage of natural healing mechanisms for patients unable to undergo traditional and more invasive treatment options.

A spectrum of vessel network architectures has been identified in animal models of chronic ischemia, ranging from heavily ramified arcades to unconnected dendritic trees, Figure 2 [14]. Animals with heavily ramified arcades show faster recovery rates and decreased tissue damage in response to ischemic insult [14-15]. Collateral vessels play a key role in this recovery by remodeling in response to an occlusion and mitigating loss of blood flow [9, 14, 15]. The collateral vessels undergo arteriogenesis, which increases diameter and the number of smooth muscle cells surrounding the vessel, allowing for an increase in flow through the vessel and greater control of the flow through it. Understanding of how these vessel's location, density, and adaptability over time affect recovery is still being investigated.

Models of the extreme ends of the vascular network spectrum are used to study the role of collateral networks in recovery from ischemic insult. Two strains of mice that represent opposing ends of the spectrum in the spinotrapezius are the Balb/C and C57Bl/6. Balb/C mice exhibit dendritic network architecture, Figure 3B; whereas C57Bl/6 mice have heavily ramified networks, Figure 3A [14]. This difference in network topology plays a critical role in susceptibility to ischemic insult, because arteriole-to-arteriole connections provide a measurement of how well flow can be re-directed around an occlusion [15]. Balb/C mice show little to no interconnection between arterioles feeding different sections of tissue, Figure 3A. For Balb/C mice, reperfusion of these sections of tissue was coincident with the transformation of capillaries into arterioles, which allowed increased flow from adjacent arteriolar trees to reach the section of tissue with restricted flow [14]. The vessels were presumed to be pre-existing capillaries undergoing arteriogenesis, thus supporting the hypothesis that pre-existing collateral vessels improve recovery time and reduce damage from occlusions.

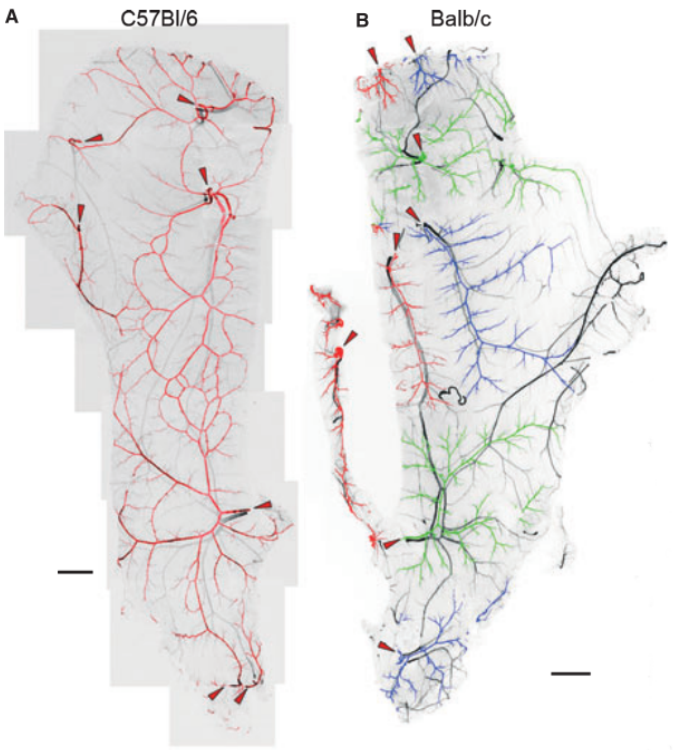

Figure 2. Differences between Balb/C and C57 network topologies. Adapted from Gabhann et al. Arteriolar and venular networks in mouse spinotrapezius muscle. C57Bl/6 shown on the left exhibits highly interconnected network. Balb/C on the right shows highly dendritic arbor with little to no interconnections [reference number].

Our collaborators have used the spinotrapezius arteriolar ligation model because it is superficial and can be whole-mounted for imaging using confocal microscopy [14]. In addition to the arterial ligation model in the spinotrapezius, the hind limb femoral artery ligation model is used to investigate the affects of collateral density on flow recovery [15]. The hind limb ligation model simulates a complete occlusion of the femoral artery, blocking downstream flow and forcing blood to travel through a collateral circuit to reach ischemic areas. Balb/C mice have fewer collateral vessels in the hind limb compared to C57s, a difference that persists for at least 21 days following femoral artery ligation [15]. This suggests Balb/C mice have a reduced capacity to remodel in response to increased flow. Strikingly, unlike in the spinotrapezius model, the gracilis muscle of Balb/C mice contains a collateral arteriole, yet downstream flow still remains impaired 21 days following femoral artery ligation [15]. This pilot study was designed to both validate previous findings and optimize a lectin perfusion stain protocol, both of which will

be used to further understand the role collateral networks in chronic flow regulation. These findings will hopefully translate into therapies that fill the gap in care for many patients suffering from PAOD.

Specific Aims and Hypothesis

This first study in this project was designed to validate the existence of collateral vessels in the gracilis muscle.

Specifc Aim 1: *To test the hypothesis that collateral arterioles are present in the gracilis muscle of Balb/C mice.* The purpose of this aim is to validate previous research and begin answering the questions of whether the spinotrapezius muscle and gracilis muscle exhibit different network topologies, whether network architecture is a limiting factor in flow recovery, and whether network remodeling is impaired or delayed compared to other strains of mice.

This second study in this project was designed to optimize the lectin perfusion stain for use in the MAVR lab.

Specific Aim 2: *To test the efficacy of lectin perfusion stain in spinotrapezius for use as a visual indicator of perfused tissue regions.* The purpose of this aim is to develop a visual method of identifying perfused regions of tissue. This would enable researchers to study recovery from perfusion deficits over time, by comparing perfusion of muscles at different time points following an occlusive event. This can be adapted to the hind-limb ligation model in the gracilis to observe changes in flow throughout the muscle following ligation.

Methods

Animal Housing and Care

Male Balb/C mice from Taconic Farms aged seven to nine weeks were used for all experiments according to protocols reviewed and approved by the California Polytechnic State University Institutional Animal Care and Use Committee. Mice were housed in a temperature-controlled room with 12-hour light and dark cycles. Mice were checked daily to ensure proper food and water levels, which were administered *ad libitum*. Cages housed 2-4 mice with bedding and enrichment devices and were changed weekly to ensure a clean environment.

Femoral Artery Ligation

The mice were anesthetized with isofluorine (1-2% flowing at 0.5-1.0 $l \cdot min^{-1}$). Hair around incision site was removed with depilatory cream and disinfected with Nolvasan. A subcutaneous injection of buprenorphrine (0.075 $mg \cdot kg^{-1}$) was then administered as an analgesic. The temperature of the mice was maintained at 35± 1.0 ° C throughout the procedure using a rectal-temperature controlled heating pad.

A skin incision was made in the medial aspect of the thigh and extended cranially and medially along femoral artery until the abdominal wall. Blunt dissection was used to remove connective tissue and expose the neurovascular bundle. The epigastric fat pad superficial the profunda femoris artery was removed and the epigastric artery-vein pair cauterized. The femoral artery was separated from the vein and nerve, then ligated downstream of the profunda femoris artery and upstream of the popliteal branch using 6-0 silk suture. Sterile saline was used throughout the procedure to irrigate the tissue and prevent muscle desiccation.

Lectin Perfusion Labeling

To visualize perfused regions of vasculature in the gracilis muscle, fluorescently labeled lectin was injected into anesthetized mice. The jugular vein of the mice was exposed and 250uL of lectin-PBS solution (concentration: 0.1mg/mL; 25ug lectin) was slowly injected using a 27-gauge insulin syringe. Pressure was briefly applied to the vein following withdrawal using a cotton swab to prevent hemorrhage.

Harvesting of Wholemount tissues:

The ipsilateral and contralateral gracilis anterior muscles were perfusion fixated (4%-paraformaldehyde solution), stripped of fascia, undermined, excised, and post-fixed overnight at 4 °C. The muscles were then rinsed and stored in PBS.

Alpha Smooth Muscle Actin Stain

To visualize arteriolar network structure of the muscle, alpha smooth muscle actin (ASMA) was stained. Muscles were removed and placed in a 24-well culture plates. The muscles were incubated for 72 hours in a solution of 1:200 1A4 clone (alpha-smooth muscle actin antibody conjugated to Cy3; Sigma, St. Louis, MO) in 0.1% saponin (reconstituted in PBS) and 2% BSA (reconstituted in PBS). The muscles were then washed in 0.1% saponin (reconstituted in PBS) 3x for 20 minutes. Following this, a final wash in PBS for 30 minutes was performed. The muscles were then whole mounted on a glass slides in a solution of 50/50 PBS and Glycerol, and then sealed with a coverslip using clear nail polish.

Imaging

All muscles were imaged using an Olympus FluoView confocal microscope, Figure 3. For optimal resolution, individual sections of the muscle were imaged and then merged to provide a whole-network view. For the ASMA stains, the collateral vessels were then examined and traced using the GNU Image Manipulation Program (GIMP). More detailed information available in Appendix C.

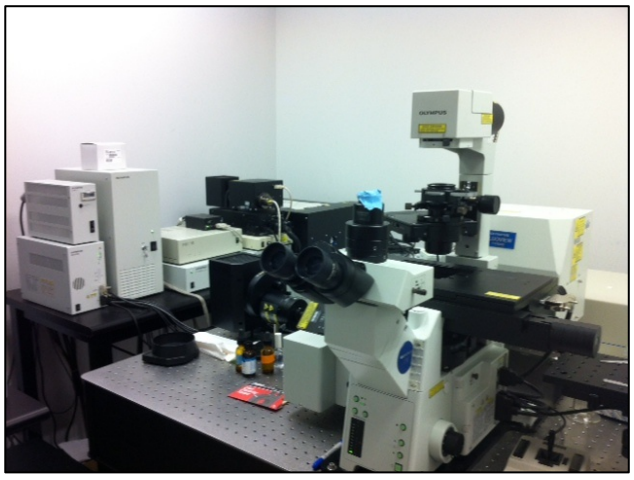

Figure 3. A layout of the confocal microscope. Microscope set-up showing the imaging apparatus and laser housing.

Results

To test the hypothesis that collateral vessels were not present in the gracilis anterior of Balb/C mice, the muscles from three mice were resected and stained following a unilateral femoral artery ligation. From the three ligated mice, one replicate was labeled as a poor stain and excluded from the analysis. The collateral network of each gracilis muscle was analyzed by hand to determine whether a collateral vessel connected the profunda artery and saphenous artery. Collateral arterioles were present in all muscles.

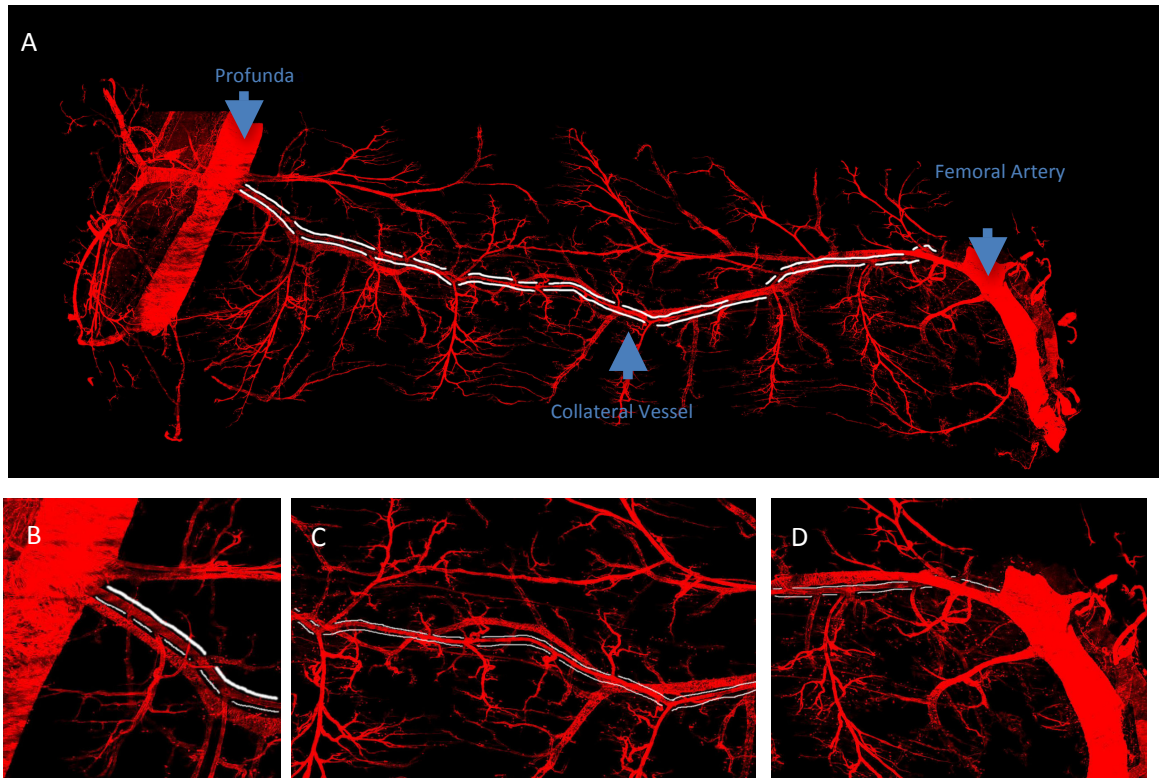

Figure 4. ASMA stain of gracilis collateral network. A) A representative image of a Balb/C collateral network in the gracilis anterior, a vessel spanning the entire muscle is shown above. B) Enlarged view of vessel branching off of the Profunda. C) Midzone of view of muscle. D) Reentry of vessel into Femoral Artery.

Mapping the network architecture lays the foundation for understanding changes in the vasculature over time. Measuring the perfusion of blood throughout the muscle under changing conditions, such as at rest and following an ischemic insult, is one of the next areas of investigation. The lectin perfusion stain performed as a first-step towards this goal. Adapting the lectin perfusion stain for use in the gracilis required first demonstrating success in replicating the previously-established protocol for perfusion imaging of the spinotrapezius. Shown is a section of spinotrapezius muscle that has been stained using the lectin perfusion technique, Figure 5.

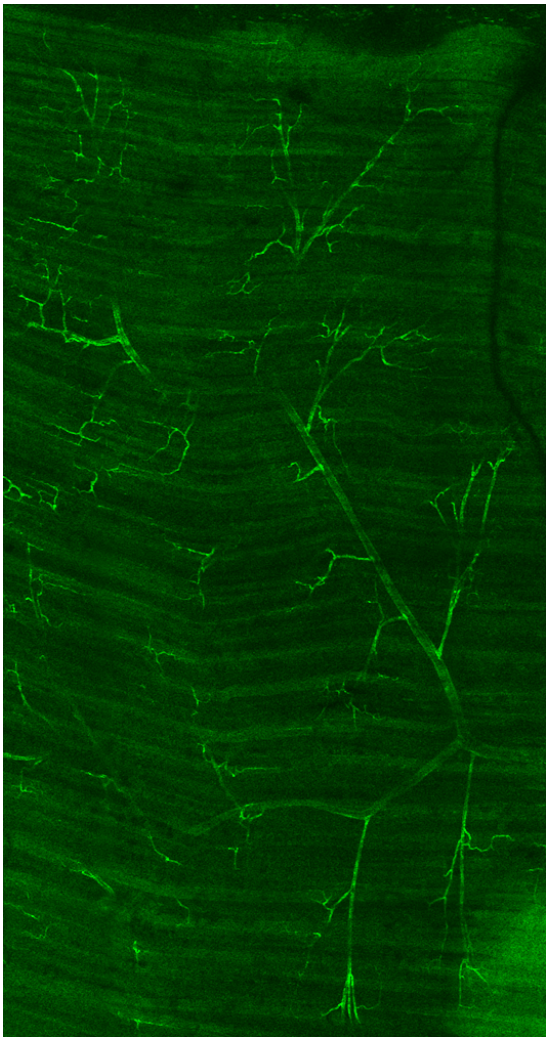

Figure 5. Lectin perfusion stain of a section of the spinotrapezius muscle. The image above shows a perfused region of the spinotrapezius microcirculation stained with lectin.

Discussion

PAOD is a worldwide disease affecting 200 million people and treatment options available to patients unable to undergo conventional surgical and endovascular treatments are limited [16, 17]. Therapies that stimulate the body's natural healing mechanisms are now being pursued to meet this need. Arteriogenesis plays a significant role in chronic regulation of the blood flow throughout the body and is a target for potential therapies [9, 12, 22]. Animal studies indicate that vascular network morphology may play a role in both the recovery time and effectiveness of innate arteriogenic healing response following an occlusion [12-13]. A notable example of this can be seen in the different recovery times experienced by Balb/C and C57 strains of mice following arterial ligation in the spinotrapezius and hind limb [12-13]. In the spinotrapezius, there are distinct differences in network topology between Balb/C and C57 strains of mice, in which the Balb/C mice exhibit highly dendritic network while the C57 has a heavily ramified structure [14]. Collateral vessels are more prevalent in the hind limb, however there are 35% fewer collaterals in the Balb/C as compared to the C57 [15]. In the spinotrapezius, immediately following arterial ligation of feed arteries supplying of dendritic microvascular networks, the arterial tree downstream of blocked feed arteries was not perfused, indicating no collaterals were present [14]. This model seems to explain the increased recovery time and decreased perfusion rates seen in the Balb/C versus the C57. However, the hindlimb also exhibited decreased perfusion and increased recovery time, despite the presence of collateral vessels in the gracilis muscle of Balb/C mice, indicating other factors other than the presence of collateral vessels may influence recovery.

Preliminary results confirm the existence of a collateral network in the Balb/C gracilis muscle as reported previously [15]. This supports the hypothesis that vascular remodeling is either impaired or delayed in Balb/C mice. Based upon this conclusion, there are multiple divergent lines of inquiry that arise. The first question stems from the time points used by Faber et al. The longest time point measured was 21 days following ligation, at which point the diameter of vessels in the collateral midzone of C57 mice had increased 143% compared to baseline versus the Balb/C mice that only experienced a 70% increase [15]. If there is a delayed response in Balb/C mice, then a later time point, such as 35 days, may show Balb/C mice with similar vessels diameters. It is also possible that the arteriogenesis process is fundamentally

impaired. The increase in diameter of vessels as compared to baseline indicates that arteriogenesis is occurring, however one or more of the signaling factors may be defective in this process. Examining monocyte recruitment following femoral artery ligation would be one place to begin investigating. Monocytes are important in the artiogenic process because after being recruited into the collateral wall, they mature into macrophages, which play a pivotal role in the vascular remodeling response [10]. Staining for the presence of these cells following femoral artery ligation would provide confirmation that either monocytes are not present, and therefore cannot initiate the arteriogenic process, or if they are, that cell signaling downstream of the monocytes may be impaired. While impaired arteriogenesis may play a role in the differences seen in recovery between C57 and Balb/C mice, the issue may be compounded by differences in collateral density as well.

Collateral density provides a metric for the number of alternate paths blood can travel to reach tissue. The greater the number of paths, the more likely flow will not be reduced to a pathological level following an occlusive event [14]. Balb/C mice have a lower collateral density in the hind limb than C57's, however whether collateral density is a major factor in chronic recovery remains to be seen [15]. One method of indirectly measuring the role of collateral density in flow recovery would be to stimulate arteriogenesis in the gracilis muscle, and observe its effect on downstream perfusion in the gastrocnemius. If flow were greatly restored, it would suggest that collateral density does not play a major role in perfusion restoration, and the only a small number of primary collaterals are needed to enlarge.

A limitation of this pilot study is the low number of replicates used (n=3). Although all mice exhibited collateral vessels, a greater number of replicates is needed to increase confidence in the results. Additionally, one replicate was excluded from the analysis due to poor visualization of the stain.

As seen throughout this paper, the ability to measure blood flow is vital to understanding recovery from an occlusive event. The lectin perfusion stain is an experimental technique that provides network-wide visualization of perfused regions of tissue at a given time and a protocol was successfully adapted from Gabhann et al. for use in this project. A critical step in ensuring the effectiveness of this process is to remove as much blood from the tissue as possible, accomplished in this protocol using perfusion fixation, as blood has a strong autofluorescence that greatly increases the amount of noise in fluorescence microscopy. This

technique has strong potential for measuring the change in perfused area of a tissue over time in the spinotrapezius, and possible applications in the gracilis muscle if properly adapted.

In summary, the pilot study and development of the lectin perfusion stain were designed to further investigate the role of the vascular architecture in the healing response following an occlusive event. The pilot study specifically focused on characterizing the network topology of the gracilis muscle in Balb/C mice. The lectin perfusion stain was adapted for use in the spinotrapezius for use in future studies. This research will hopefully lead to therapies that fill unmet needs for patients suffering from PAOD.

References:

[1] J. F. Lau, M. D. Weinberg, and J. W. Olin, "Peripheral artery disease. Part 1: clinical evaluation and noninvasive diagnosis.," *Nature reviews. Cardiology*, vol. 8, no. 7. pp. 405–18, Jul-2011.

[2] A. T. Hirsch, Z. J. Haskal, N. R. Hertzer, C. W. Bakal, M. a Creager, J. L. Halperin, L. F. Hiratzka, W. R. C. Murphy, J. W. Olin, J. B. Puschett, K. a Rosenfield, D. Sacks, J. C. Stanley, L. M. Taylor, C. J. White, J. White, R. a White, E. M. Antman, S. C. Smith, C. D. Adams, J. L. Anderson, D. P. Faxon, V. Fuster, R. J. Gibbons, S. a Hunt, A. K. Jacobs, R. Nishimura, J. P. Ornato, R. L. Page, and B. Riegel, "ACC/AHA 2005 Practice Guidelines for the management of patients with peripheral arterial disease (lower extremity, renal, mesenteric, and abdominal aortic): a collaborative report from the American Association for Vascular Surgery/Society for Vascular Sur," *Circulation*, vol. 113, no. 11, pp. e463–654, Mar. 2006.

[3] M. a Ziegler, M. R. Distasi, R. G. Bills, S. J. Miller, M. Alloosh, M. P. Murphy, a G. Akingba, M. Sturek, M. C. Dalsing, and J. L. Unthank, "Marvels, mysteries, and misconceptions of vascular compensation to peripheral artery occlusion.," *Microcirculation*, vol. 17, no. 1, pp. 3–20, Jan. 2010.

[4] P. Libby, P. M. Ridker, and G. K. Hansson, "Progress and challenges in translating the biology of atherosclerosis.," *Nature*, vol. 473, no. 7347, pp. 317–25, May 2011.

[5] M. Al-Qaisi, D. M. Nott, D. H. King, and S. Kaddoura, "Ankle brachial pressure index (ABPI): An update for practitioners.," *Vasc. Health Risk Manag.*, vol. 5, pp. 833–41, Jan. 2009.

[6] a. T. Hirsch, S. L. Halverson, D. Treat-Jacobson, P. S. Hotvedt, M. M. Lunzer, S. Krook, S. Rajala, and D. B. Hunninghake, "The Minnesota Regional Peripheral Arterial Disease Screening Program: toward a definition of community standards of care," *Vasc. Med.*, vol. 6, no. 2, pp. 87–96, May 2001.

[7] D. P. Slovut and E. C. Lipsitz, "Surgical technique and peripheral artery disease.," *Circulation*, vol. 126, no. 9, pp. 1127–38, Aug. 2012.

[8] M. D. Weinberg, J. F. Lau, K. Rosenfield, and J. W. Olin, "Peripheral artery disease. Part 2: medical and endovascular treatment.," *Nature reviews. Cardiology*, vol. 8, no. 8. pp. 429–41, Aug-2011.

[9] A. Helisch and W. Schaper, "Arteriogenesis: the development and growth of collateral arteries.," *Microcirculation*, vol. 10, no. 1, pp. 83–97, Jan. 2003.

[10] M. Heil, I. Eitenmüller, T. Schmitz-Rixen, and W. Schaper, "Arteriogenesis versus angiogenesis: similarities and differences.," *J. Cell. Mol. Med.*, vol. 10, no. 1, pp. 45–55, 2006.

[11] M. Potente, H. Gerhardt, and P. Carmeliet, “Basic and therapeutic aspects of angiogenesis.,” *Cell*, vol. 146, no. 6, pp. 873–87, Sep. 2011.

[12] A. J. LeBlanc, L. Krishnan, C. J. Sullivan, S. K. Williams, and J. B. Hoying, “Microvascular repair: post-angiogenesis vascular dynamics.,” *Microcirculation*, vol. 19, no. 8, pp. 676–95, Nov. 2012.

[13] R. Gupta, J. Tongers, and D. W. Losordo, “Human Studies of Angiogenic Gene Therapy,” *Circ. Res.*, vol. 105, no. 8, pp. 724–736, Oct. 2009.

[14] F. Mac Gabhann and S. M. Peirce, “Collateral capillary arterialization following arteriolar ligation in murine skeletal muscle.,” *Microcirculation*, vol. 17, no. 5, pp. 333–47, Jul. 2010.

[15] D. Chalothorn, J. a Clayton, H. Zhang, D. Pomp, and J. E. Faber, “Collateral density, remodeling, and VEGF-A expression differ widely between mouse strains.,” *Physiol. Genomics*, vol. 30, no. 2, pp. 179–91, Jul. 2007.

[16] D. P. Slovut and T. M. Sullivan, “Critical limb ischemia: medical and surgical management.,” *Vasc. Med.*, vol. 13, no. 3, pp. 281–91, Aug. 2008.

[17] D. Scholz, “Contribution of Arteriogenesis and Angiogenesis to Postocclusive Hindlimb Perfusion in Mice,” *J. Mol. Cell. Cardiol.*, vol. 34, no. 7, pp. 775–787, Jul. 2002.

[18] G. Gruionu, J. B. Hoying, A. R. Pries, and T. W. Secomb, “Structural remodeling of mouse gracilis artery after chronic alteration in blood supply,” vol. 5051, pp. 2047–2054, 2005.

APPENDIX A

B

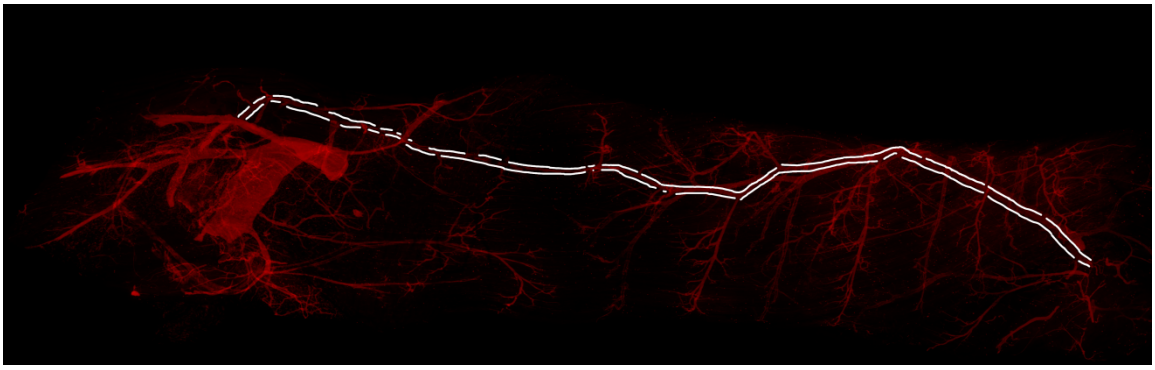

Figure 6. 3.7.13 Left non-ligated

C

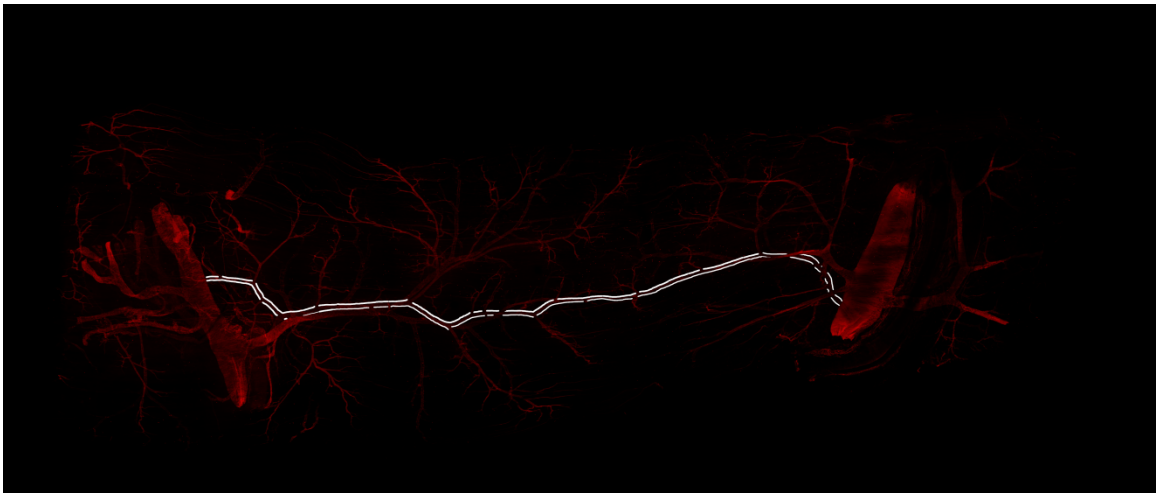

Figure 7. 3.11.13 left ligated

D

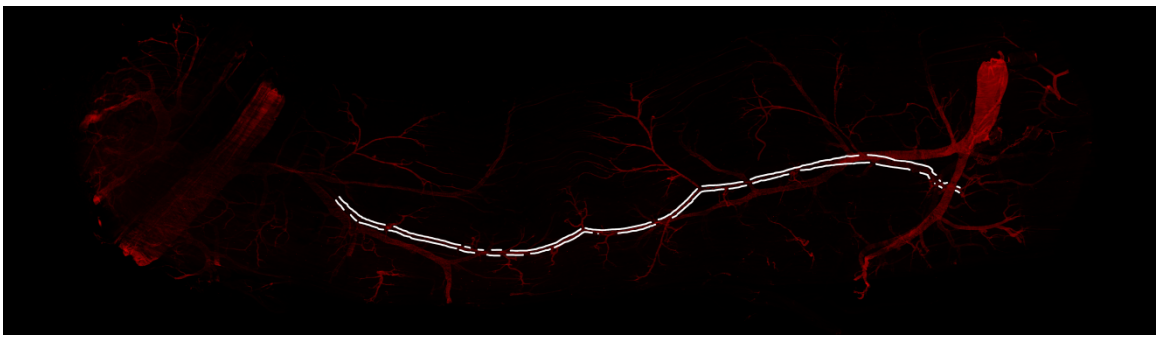

Figure 8. 3.11.13 Right non ligated

APPENDIX B

Femoral Artery Ligation Protocol

Date_____ **Hindlimb Ischemia Surgery - Ligation** Initials_____

Mouse Information
DOB:_____
Sex:_____
Tag:_____
Genotype/strain:_____
Cage:_____

Materials
Sterilize- autoclave or flash autoclave
____1. forceps (2)
____2. fine forceps (2)
____3. ultrafine forceps (1)
____4. fine scissors (1)
____5. microscissors spring loaded (1)

Pre-sterilize in autoclave
____6. cotton gauze (2)
____7. cotton swabs (12)
____8. 6.0 silk suture (2 x 1-inch)
____9. needle holder (1)

Obtained in surgery suite
____10.sterile Petri dish w/ sterile saline
____11.sterile gloves
____12.sterile 7.0 prolene suture
____13.heat-cautery
____14.FST heat pad w/ rectal probe
____15.heat pad
____16.recovery bin & weigh boat
____17.depilatory cream
____18.non-sterile cotton swabs
____19.non-sterile cotton gauze
____20.isolation mask & cap
____21.analgesic (Buprenorphine)

Surgery preparation
____22.Spray surgery area with Nolvasan
____23.Weigh animal in weight boat
____24.Place animal in anesthesia box
____25.Open the oxygen cylinder and set anesthesia-machine flow meter to ~3 $l \cdot min^{-1}$
____26.Anesthetize animal w/ 5% isoflurane
____27.Affix non-rebreathing circuit to bench-top with tape
____28.Reduce flow rate to 0.5-1.0 $l \cdot min^{-1}$ and the isoflurane to 1-3%
____29.Apply ear tag high on left ear
____30.Lay animal supine with nose in nose-cone
____31.Shave hair on the right hindlimb & lower abdomen with clippers
____32.Remove excess hair with depilatory cream
____33.Spray right hindlimb with Nolvasan
____34.Return animal to anesthesia box
____35.Apply 4x4 gauze sponge to heat pad to protect animal from excessive heat
____36.Affix non-rebreathing circuit to surgery table w/ chemistry clamp
____37.Lay animal supine on circulating heat pad w/ nose in nose-cone
____38.Insert rectal probe and set thermo-controller to 37°C
____39.Apply veterinary ointment to eyes to avoid drying during procedure
____40.Apply veterinary ointment to anus and place rectal probe ~1cm into anus to monitor core-body temperature

Surgery
____41.Make a small incision on the middle, medial aspect of the left thigh
____42.Extend the incision up to the abdominal wall
____43.Blunt dissect the subcutaneous connective tissue to maximize surgical exposure
____44.Use cautery to remove fat pad overlying femoral a-v pair & cauterize epigastric av-pair
____45.Blunt dissect the femoral artery from the neurovascular bundle just downstream from the deep femoral branch
____46.Tie off the femoral artery & vein with 6.0 silk suture, just downstream to the deep femoral branch
____47.Use 6.0 polypropylene suture to close the skin
____48.Make a small incision on the middle, medial aspect of the right thing
____49.Extend the incision up to the abdominal wall
____50.Blunt dissect the subcutaneous connective tissue to maximize surgical exposure
____51.Use 6.0 polypropylene suture to close the skin

Post-Surgical
____52.Give the animal an subcutaneous injection of buprenorphine (0.075mg/kg)
____53.Place the animal in the recovery bin, on a blue bench cover, above a heat pad and allow to recover
____54.Turn flow meter down to 0, turn off isoflurane, and close the oxygen cylinder
____55.Indicate surgery on cage card

Notes
_____
_____
_____
_____

Materials

24-well culture plates (Cat#: 3738, Corning Incorporated)
PBS
0.1% Saponin (Cat#: 47036, Sigma-Aldrich)
2% Bovine Serum Albumin (Cat# B6917, Sigma Aldrich)
Monoclonal Anti-Alpha Smooth Muscle Actin, Cy3 Conjugate (Cat#: C6198, Sigma-Aldrich)
Slides
Coverslips
Parafilm
Aluminum foil

Staining

1. Using forceps, remove muscle from PBS (stored in microcentrifuge tube at 4°C) and place in a single well of a 24-well culture plate.
2. Prepare antibody solution containing 1:200 1A4 clone (alpha-smooth muscle actin, Cy3 conjugate) in 0.1% saponin (reconstituted in PBS), 2% BSA (reconstituted in PBS) in PBS, using 0.3mL of solution per muscle.
3. Incubate muscle in antibody solution for 3 nights (72 hours) at 4°C). **(Note: Critical step—3 nights crucial for bright staining) by gently pipetting solution over muscle.)**
4. Wash in 0.1% saponin in PBS 3x for 20 minutes at room temperature. Cover plate with foil during each wash.
5. Wash in plain PBS for 30 minutes. Cover with foil during each wash.
6. Place 1-2 drops of 50/50 PBS and Glycerol onto slide.
7. Remove muscle from well using forceps and place on a slide.
8. Add 1-2 drops of 50/50 PBS and Glycerol to the top of the muscle and place cover slips over the muscle.
9. Paint edges of coverslip with clear nail polish to create a seal and prevent tissue desiccation.
10. Store slides at 4°C wrapped in foil or an opaque container between imaging.

Imaging

11. Image using a standard fluorescent microscope. (Cy3 excitation: 550 nm, emission: 570 nm)

APPENDIX C

Lectin Imaging

Using the FV10-ASW version 4.1 software, an outline of the muscle area in the x-y plane was described. Next, the thickness of the muscle (z-direction) was described by setting z-min to the bottom of the visible muscle and z-max to the top of the visible muscle. The automated image capture program was then initiated. The program automatically merged pictures in each x-y plane together. The collective merged images then formed a z-stack, each describing a discrete level in the z-axis. Two-dimensional images of the network were produced by averaging the z-stack of images using the ImageJ program, described in greater detail in Appendix C.

APPENDIX D

ImageJ Protocol

The z-stack of images was imported into ImageJ using the image sequence, Figure A.

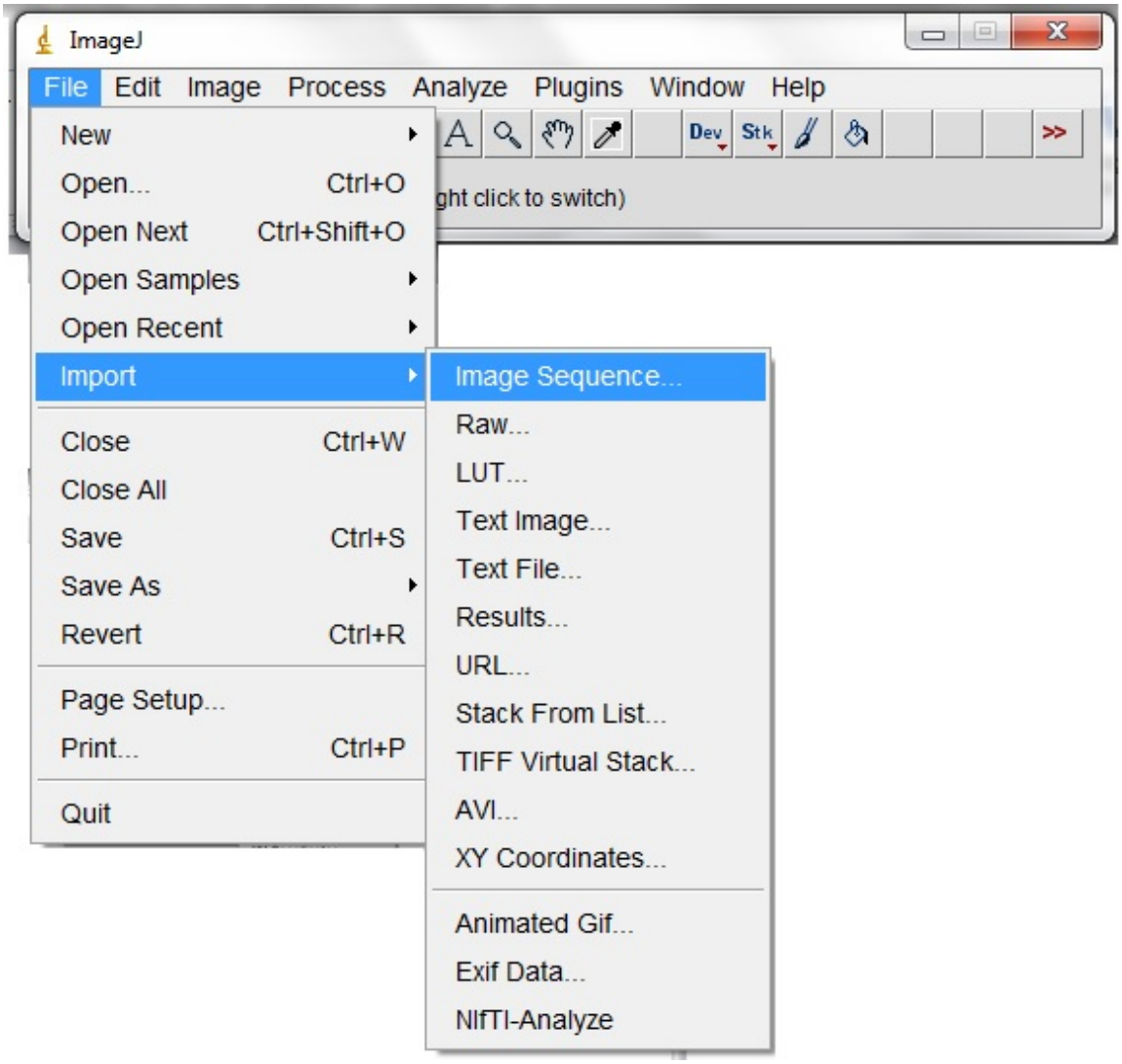

Figure A

A z-project was then created, and the sum feature was used to merge the images into a two-dimensional image and is shown in Figure B below.

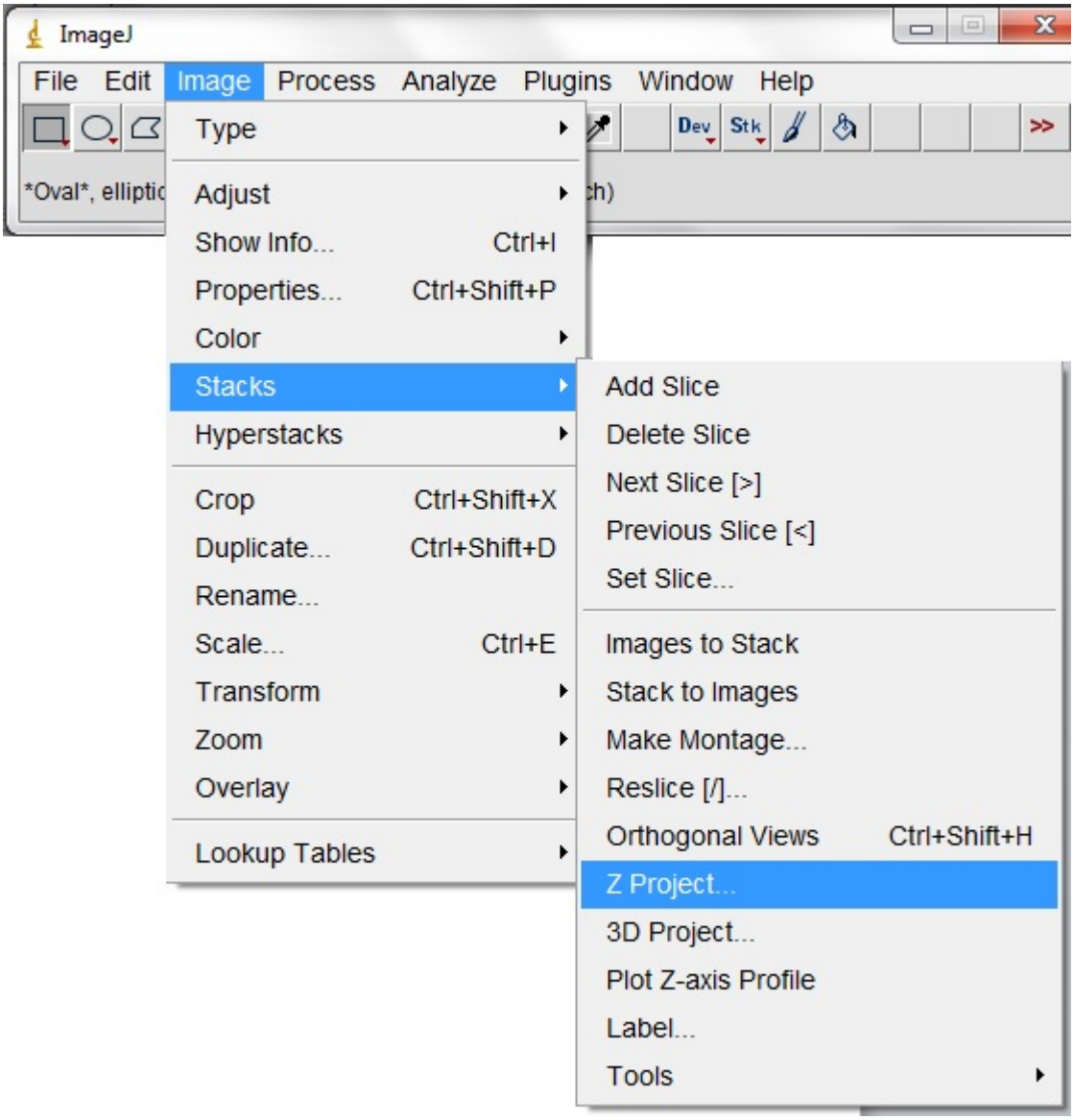

Figure B

APPENDIX E

Troubleshooting the Lectin Perfusion Stain

Adapting the lectin perfusion staining protocol for use in the gracilis presented a series of challenges. The first challenge resulted from the autofluoresence of blood occurring within the same band of wavelength as the lectin stain used, drowning out the signal from the lectin. Performing a perfusion fixation in place of in situ fixation mitigated this problem.

The next challenge was capturing a clear image of the stain. Using the widefield fluorescent microscope provided sharper resolution when viewed through the lenses, however image quality was an issue when using the attached camera. After trying to adjust the gain, autofocus, and brightness with little success the imaging was moved to the confocal microscope. Here initial results were promising, however they were later discarded when it was found using gain at 90% cuts out most of the data, and the data that remains becomes indistinguishable from noise, possibly creating an inaccurate visual description of the vessels. Gain levels below 10% were recommended.

Originally a single plane was used to capture the images, however this resulted in a loss of clarity as vessels would appear and disappear due to the 3D nature of the subject. This third dimension of the muscle was better captured by taking pictures at different heights throughout the thickness of the muscle. This introduced the complication of merging the planes into a 2D image or building a 3D model of the vessel. Building a 3D image of the vessel proved to be beyond the scope and timeframe of the project, as it was intensive in both the amount of time it took to capture the data and effort needed to analyze it.

Deciding how to merge the planes required two decisions. First was the number of “slices” the camera would take in the z-direction, to capture the thickness of the vessel. Take too many images and the noise from all of the images begins to combine and drown out the useful date. Take too few and there is a risk of missing critical vessel structures. Through trial and error a number of 10 slices was established, as it represented a good balance of time spent imaging to quality of the images. The second decision was how to merge the images from the different planes, which required some amount of manipulation of the images. The ImageJ software provided different options such as Average, Max, Min, and Sum slices to combine the stack of images. The Average function was chosen as it helped clarify vessels while not dramatically increasing the amount of noise. Functions such as Max and Sum tended to produce over saturated images that lost clarity. Overall muscle clarity still needs to be improved, as only sections of the muscle were clearly visible with the stain. This is likely due to the 3D

nature of the muscle and can be dealt with by optimizing the image capturing techniques used with the confocal microscope.